ALICE at the LHC and astrophysics: From providing input for the search for antinuclei in space to constraining the equation of state of neutron stars

Alexander Kalweit⋆ (on behalf of the ALICE collaboration)

CERN, Geneva

⋆ Alexander.Philipp.Kalweit@cern.ch

*21st International Symposium on Very High Energy Cosmic Ray Interactions
(ISVHECRI 2022)
Online, 23-28 May 2022*

Abstract

The ALICE experiment at the LHC was originally designed to study the creation of the quark-gluon-plasma in heavy-ion collisions, a new state of matter in which quarks and gluons are not confined into hadrons. More recently, the versatility of both the Large Hadron Collider and the ALICE apparatus have given additionally access to a unique set of nuclear and hadronic physics measurements. The main results from this new and dynamic research area will be presented. The application of these findings to astrophysical challenges, ranging from the equation of state of neutron stars to the search for dark matter in space, will be discussed.

1 Introduction

ALICE (A Large Ion Collider Experiment) is the LHC experiment that is optimised to study the creation and properties of the quark-gluon-plasma (QGP) [1]. The QGP corresponds to a deconfined state of matter that is created in ultra-relativistic heavy-ion collisions and that also existed in the early universe shortly after the big bang [2]. Recently, the unique particle identification and tracking capabilities of ALICE have also been utilised to provide crucial input for astrophysical challenges. In this article, two of these topics will be discussed: the search for antinuclei in space and the equation of state of neutron stars. While several intriguing results in this domain could already be established based on the LHC Run 1 and 2 data (2010-2018), many new insights are expected from the upgraded ALICE 2 detector that is currently starting the LHC Run 3 and 4 (2022-2032) campaign. The field of study presented here will profit also largely from the proposed ALICE 3 detector that is envisaged to take data towards the completion of the LHC life cycle in Run 5 and 6 (2035 and beyond).
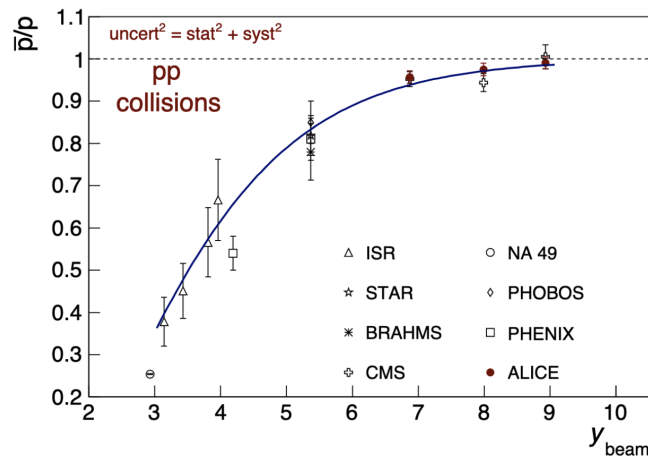
Figure 1: Antiproton to proton ratio as a function of beam rapidity. The three ALICE measurements correspond to $\sqrt{s}$ =0.9, 2.76, and 7 TeV. Figure taken from [3].

2 ALICE and the search for antinuclei in space

The search for antinuclei in space is mainly motivated by the fact that they are sensitive probes of weakly interacting massive particles (WIMP) in dark matter searches. If they existed, they would accumulate in the centre of our galaxy where they potentially annihiliate into antinuclei such as $^3\overline{\text{He}}$.

For collider based experiments such as ALICE, this essentially poses three challenges to address. Firstly, to understand the antinuclei formation processes in order to model their occurrence in dark matter annihilation and subsequent decays. Secondly, to quantitatively asses the production of antinuclei in background reactions, i.e. in the collisions of energetic cosmic rays. Thirdly, to study the interaction of antinuclei with matter particles in order to determine the transparency of the galaxy.

2.1 Antinuclei production and coalescence models

As a matter of fact, the LHC is ideally suited for such studies as it can serve as an antimatter factory. Thanks to its very high energy, antiparticles and particles are produced in essentially equal abundance at midrapidity. For instance, the antiproton-to-proton ratio ($\overline{\text{p}}/\text{p}$) in pp collisions at $\sqrt{s} = 7$ TeV has been determined as $0.991 \pm 0.005\,(stat.) \pm 0.014\,(syst.)$ [3].

For heavier antiparticles with mass number A, one finds similar values in line with the coalescence and thermal model expectation of $(\overline{\text{p}}/\text{p})^A$ [4]. Nevertheless, the production of heavier antinuclei remains quite rare: only roughly 2% of all produced particles are antiprotons [5] and for each additional antinucleon, a penalty factor of around 350 for Pb-Pb and around 1000 for pp collisions applies [4, 6, 7]. This exponential decrease of the particle yield with increasing mass number of the antinucleus is illustrated in Fig. 2.

Over the last years, ALICE delivered a unique set of high-quality data on antinuclei production for various collision systems ranging from pp, to p–Pb, and Pb–Pb collisions. In many cases, this data is interpreted on the basis of statistical-thermal [8–10] and coalescence models [11–15]. For astrophysical purposes as discussed here, the coalescence model is mostly used to describe antinucleus formation based on antiprotons and antineutrons that are close by in momentum and configuration space. Since antiprotons and antineutrons are expected to be produced in equal abundance at LHC energies, the antideuteron invariant yield $E_d \frac{\text{d}^3 N_d}{\text{d}p_d^3}$ is then, for example, given by
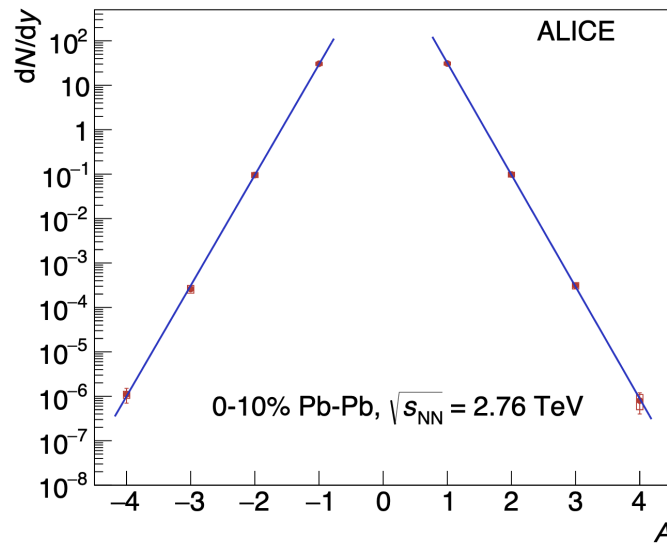
Figure 2: Transverse momentum integrated yield $\mathrm{d}N/\mathrm{d}y$ per unit rapidity at midrapidity for various light nuclei and antinuclei as a function of the mass number A. Figure taken from [7].

$$E_d \frac{\mathrm{d}^3 N_d}{\mathrm{d}p_d^3} = B_2 \left(E_p \frac{\mathrm{d}^3 N_p}{\mathrm{d}p_p^3} \right)^2 , \tag{1}$$

where $E_p \frac{\mathrm{d}^3 N_p}{\mathrm{d}p_p^3}$ corresponds to the antiproton yield and the proportionality factor is the so-called coalescence parameter B_2. In reality, the latter is a complicated function of the Wigner function of the produced antinucleus folded with the particle emitting source (see [12,13] for details). However, for practical purposes it is often implemented as an afterburner in event generators in which two antinucleons are coalesced if their momentum difference is smaller than a typical scale of $p_0 \lesssim 100$ MeV. At first glance, this momentum scale seems large with respect to the small binding energy of 2.2 MeV of the antideuteron. However, if one considers that the kinetic energy of an antinucleon with a momentum of 100 MeV corresponds only to 5.3 MeV, the process indeed becomes plausible. Figure 3, shows a compilation from [16] of recent antideuteron and deuteron measurements for various collision systems compared to a coalescence [17] and thermal-statistical model [10].

Many astrophysics groups then fit their models to the existing B_2 measurements and calculate the existing antideuteron or antihelion fluxes near Earth (for two recent examples see for instance [18–20]). In these calculations, one typically finds that the expected flux of $^3\overline{\mathrm{He}}$ near Earth for essentially all dark matter models is below the current sensitivity of the AMS-02 experiment which is in contrast to the reporting of a few potential candidates by the AMS-02 collaboration.

One of the most interesting recent developments in this context is therefore the possible enhancement of the $^3\overline{\mathrm{He}}$ signal from dark matter via their formation in $\overline{\Lambda}_b^0$ decays as shown by Winkler and Linden in [21]. Also in this case, accelerator based experiments are required to determine the branching ratio of the $\overline{\Lambda}_b^0 \to {}^3\overline{\mathrm{He}} + X$ decay. The decay is schematically illustrated in Fig. 4 and model estimates from various PYTHIA and HERWIG tunes indicate a value of the branching ratio in the 10^{-5} to 10^{-9} range [21].

Experimentally, it will be studied with the current and future ALICE detectors by investigating $^3\overline{\mathrm{He}}$ from displaced origin. Due to the lifetime of $c\tau \approx 441\ \mu$m of the $\overline{\Lambda}_b^0$, those $^3\overline{\mathrm{He}}$
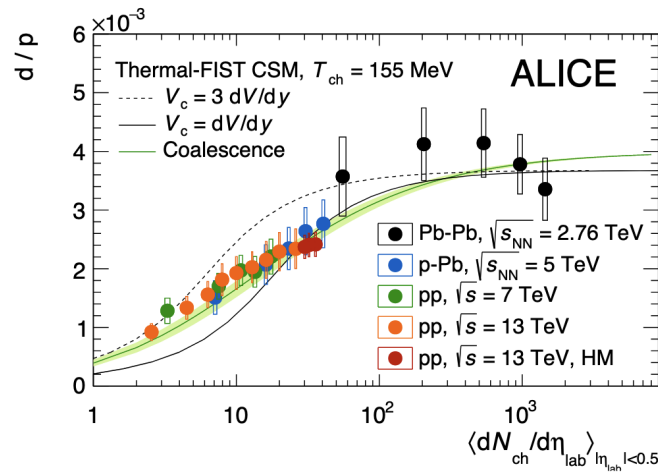
Figure 3: Deuteron over proton ratio for various collision systems as a function of the number of charged particles produced in the event. The data is compared to a coalescence [17] and a thermal-statistical [10] model. Figure taken from [16].
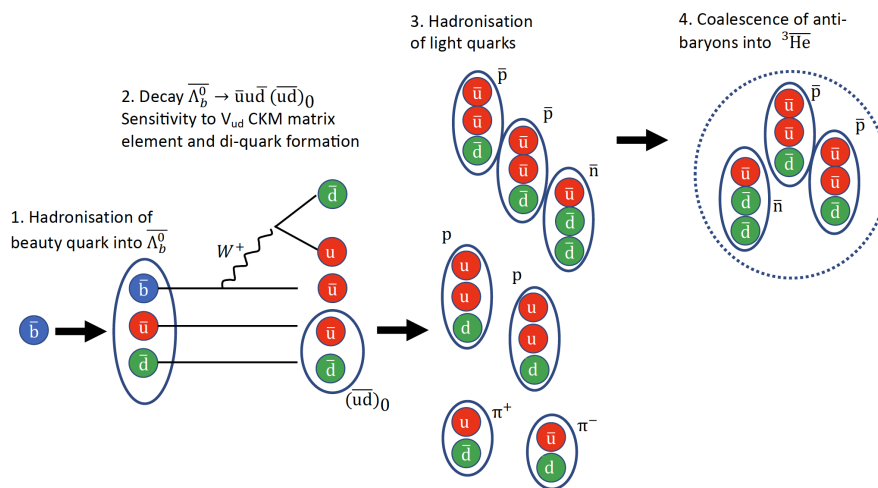
Figure 4: Schematic illustration of $^3\overline{\text{He}}$ formation in $\overline{\Lambda}_b^0$ decays.

originating from $\overline{\Lambda}_b^0$-decays populate the tails of the distribution of the distance of closest approach to the primary interaction vertex. As shown in Fig. 5, a clear separation between these two contributions will be already achieved with a further upgrade of the Inner Tracking system of ALICE (ITS3), but an ultimate performance will be reached with the planned ALICE 3 detector that envisages a tracking layer inside the beampipe [22]. This will either allow for a measurement of or an upper limit on the branching ratio in the 10^{-7} to 10^{-6} range after LHC Run 4 and in 10^{-8} range after LHC Run 5.

2.2 Transparency of the galaxy to antinuclei

In order to determine the transparency of our galaxy to antinuclei, the inelastic cross-sections for the interaction of antinuclei with matter need to be determined. This is best illustrated with the following back-of-the-envelope estimate for the mean free path λ of an antinucleus
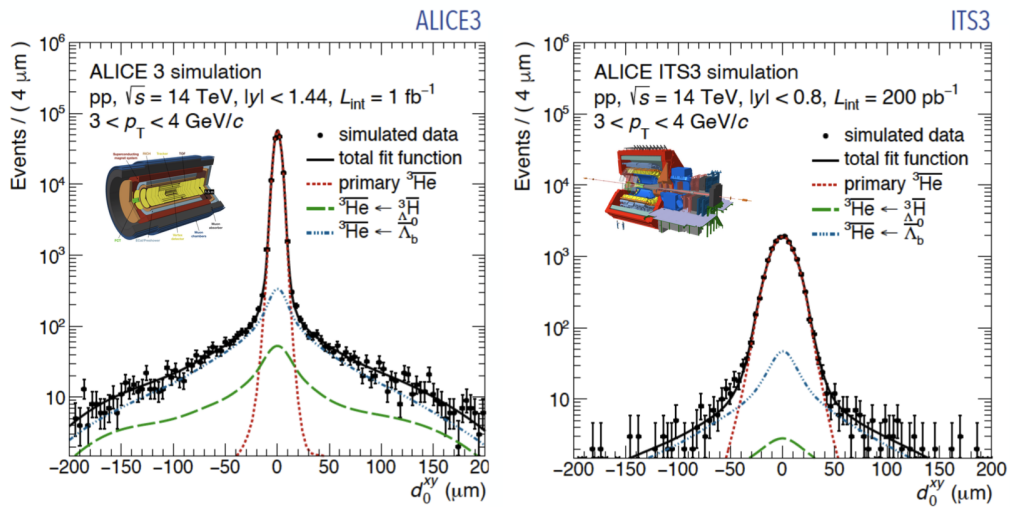
Figure 5: Simulation of the distribution of the distance of closest approach to the primary vertex for $^3\overline{\text{He}}$ particles of either primary or secondary origin. Results are shown for the ALICE 3 (left) and ITS3 (right) detector that will be installed in LHC Run 5 and 4, respectively. The astrophysically relevant signal is the dashed dotted line that indicates those $^3\overline{\text{He}}$ which stem from $\overline{\Lambda}^0_b$-decays. Figure taken from [22].

in the galaxy,

$$\lambda = \frac{1}{n \cdot \sigma}, \qquad (2)$$

where n corresponds to the number density of particles in the galaxy and σ to the interaction cross-section. If one plugs in some rough numbers such as three hydrogen and helium atoms per cubic centimetre $n \approx 3/\text{cm}^{-3}$ and $\sigma \approx 2\,\text{b} = 2 \cdot 10^{-24}\text{cm}^{-2}$, one indeed obtains a distance of roughly 180000 light years, thus of the order of the diameter of the Milky Way. In reality, the trajectory of antinuclei through the galaxy does not occur on straight lines due to the presence of magnetic fields and is thus larger. The latter point is addressed by the usage of propagation codes such as GALPROP [23] and the second ingredient, that is given by the cross-section, has been measured by the ALICE collaboration as explained in the following.

In fact, the inelastic interaction cross-sections of antinuclei remained poorly known until the recent efforts by the ALICE collaboration: only two papers on antideuteron cross-sections at high momenta were published in the 1970s [24, 25]. This is due to the fact that beams of heavier antinuclei are very difficult to obtain. In two recent ALICE analyses, the ALICE detector itself was therefore used as a target [26, 27]. Antinuclei produced in a collision in the centre of ALICE travel through the various subdetector components. Both the Time Projection Chamber (TPC) and the Time of Flight (TOF) detectors can unambiguously identify $^3\overline{\text{He}}$. By counting those arriving in the outwards TOF with respect to those exiting the inwards TPC, one directly obtains the absorption cross-section for the average material in between these detectors. After extrapolating these cross-sections to hydrogen and helium targets, these cross-sections can be fed into propagation codes. By calculating the ratio of the $^3\overline{\text{He}}$-flux with the experimentally constrained cross-sections to the flux where these are set equal to zero, we obtain the transparency. For a typical Dark Matter signal such as a WIMP with 100 GeV/c^2 mass decaying into W^+W^- pairs, a rather constant transparency as a function of the kinetic energy of the $^3\overline{\text{He}}$ nucleus is found. It amounts to about 50% for the signal and to about 25%–90% for the background [27].
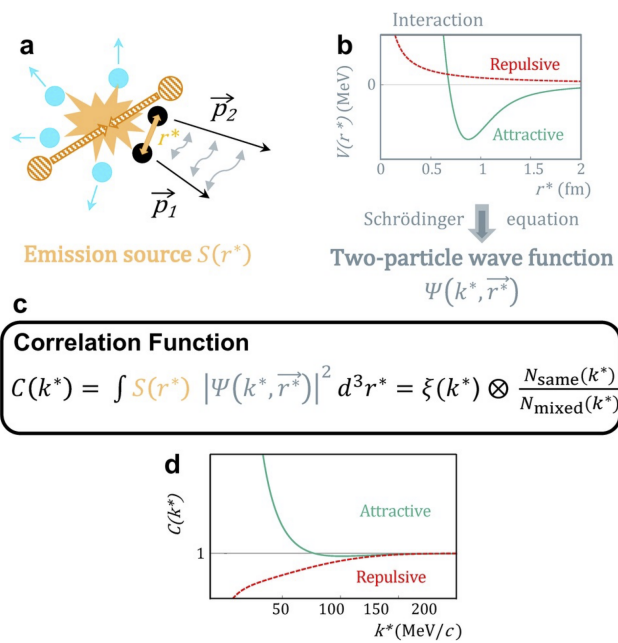
Figure 6: The collision of two protons in the LHC creates among other particles a pair of hadrons that is close-by in phase space (a). Their interaction potential (b) defines the resulting correlation function (c). The latter is increasing for small relative momenta $\vec{k}^*$, if the interaction is attractive and decreasing, if the interaction is repulsive (d). Figure taken from [30].

3 ALICE and the equation of state of neutron stars

Neutron stars are among the most fascinating objects in our universe. Nevertheless, the composition of the innermost core of neutron stars is still unknown. With increasing baryonic densities, the production of hyperons becomes energetically more favourable and they could appear in such environments depending on the strength of two and three body hyperon-nucleon and hyperon-hyperon interactions [28,29]. The appearance of strange hadrons leads to a softening of the equation of state and this has a direct impact on the mass-radius relation.

In ALICE, the residual strong interaction between two hadrons is accessible via the so-called femtoscopy technique. This innovative approach is conceptually illustrated in Fig. 6. Proton-proton collisions at the LHC produce several hadrons of various species per collision that are emitted in various directions. In some cases, two hadrons are emitted close-by in phase-space and they fly next to each other for many femtometers. If their interaction is attractive, this leads to an enhancement of the correlation function at small momentum differences, because the momentum vectors of the two particles get more aligned. Likewise, if their interaction is repulsive, a depletion at small momentum differences is observed [30]. Interestingly, the interactions for the heavier multi-strange baryons can be reliably calculated ab initio using Lattice QCD [31].

As shown in Fig. 7, the attractive potential between p-Ξ and p-Ω can be well described by these calculations. This allows one to constrain the theoretically calculated interaction potentials from the experimental side. Afterwards, they can be fed back into the calculation of the equation of state of neutron stars [29].
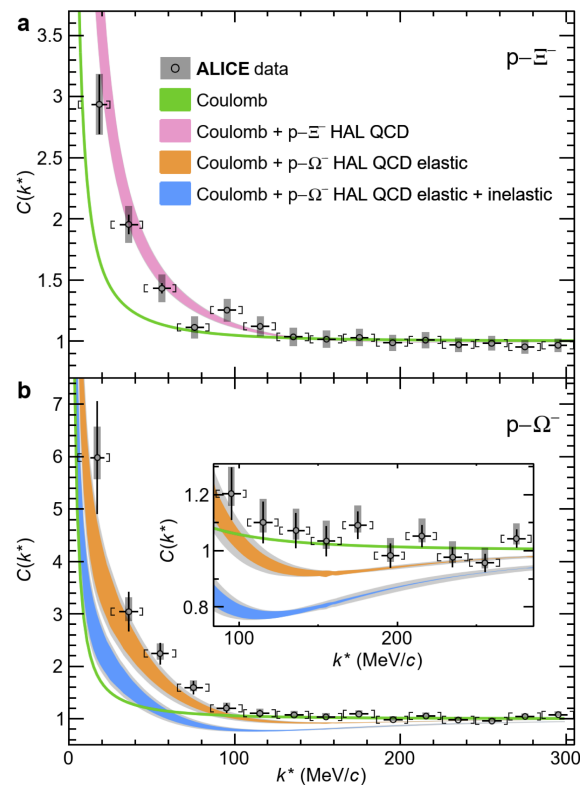
Figure 7: Two-particle correlation function as a function of transverse momentum for p-Ξ (a) and p-Ω (b) pairs compared to Lattice QCD predictions. Figure taken from [30].

4 Conclusion and Outlook

ALICE has strong PID and tracking capabilities over a large momentum range. These unique features give access not only to quark-gluon-plasma physics, but they can also be exploited for astrophysical challenges. Two main examples were discussed in this work. Firstly, the antinuclei program of ALICE that has delivered a high-quality set of data for the understanding of their production mechanism and interaction with matter. Secondly, two-particle correlation measurements that shed light on hadron-hadron interactions which constrain the equation of state of neutron stars. The upcoming runs at the LHC together with the upgraded ALICE detector will continue to provide important insights into this exciting field of research.

References

[1] K. Aamodt et al., *The ALICE experiment at the CERN LHC*, J. Instrum. **3**, S08002 (2008), doi:10.1088/1748-0221/3/08/S08002.

[2] E. V. Shuryak, *Quantum chromodynamics and the theory of superdense matter*, Phys. Rep. **61**, 71 (1980), doi:10.1016/0370-1573(80)90105-2.

[3] E. Abbas et al., *Mid-rapidity anti-baryon to baryon ratios in pp collisions at $\sqrt{s} = 0.9, 2.76$ and 7 TeV measured by ALICE*, Eur. Phys. J. C **73**, 2496 (2013), doi:10.1140/epjc/s10052-013-2496-5.

[4] S. Acharya et al., *Production of deuterons, tritons, ^3He nuclei and their antinuclei in pp collisions at $\sqrt{s}$ = 0.9, 2.76 and 7 TeV*, Phys. Rev. C **97**, 024615 (2018), doi:10.1103/PhysRevC.97.024615.

[5] S. Acharya et al., *Production of charged pions, kaons, and (anti-)protons in Pb-Pb and inelastic pp collisions at $\sqrt{s_{NN}}$ = 5.02 TeV*, Phys. Rev. C **101**, 044907 (2020), doi:10.1103/PhysRevC.101.044907.

[6] J. Adam et al., *Production of light nuclei and anti-nuclei in pp and Pb-Pb collisions at energies available at the CERN Large Hadron Collider*, Phys. Rev. C **93**, 024917 (2016), doi:10.1103/PhysRevC.93.024917.

[7] S. Acharya et al., *Production of ^4He and $^4\overline{He}$ in Pb-Pb collisions at $\sqrt{s_{NN}}$ = 2.76 TeV at the LHC*, Nucl. Phys. A **971**, 1 (2018), doi:10.1016/j.nuclphysa.2017.12.004.

[8] A. Andronic, P. Braun-Munzinger, J. Stachel and H. Stöcker, *Production of light nuclei, hypernuclei and their antiparticles in relativistic nuclear collisions*, Phys. Lett. B **697**, 203 (2011), doi:10.1016/j.physletb.2011.01.053.

[9] J. Cleymans, S. Kabana, I. Kraus, H. Oeschler, K. Redlich and N. Sharma, *Antimatter production in proton-proton and heavy-ion collisions at ultrarelativistic energies*, Phys. Rev. C **84**, 054916 (2011), doi:10.1103/PhysRevC.84.054916.

[10] V. Vovchenko, B. Dönigus and H. Stoecker, *Multiplicity dependence of light nuclei production at LHC energies in the canonical statistical model*, Phys. Lett. B **785**, 171 (2018), doi:10.1016/j.physletb.2018.08.041.

[11] S. T. Butler and C. A. Pearson, *Deuterons from high-energy proton bombardment of matter*, Phys. Rev. **129**, 836 (1963), doi:10.1103/PhysRev.129.836.

[12] R. Scheibl and U. Heinz, *Coalescence and flow in ultrarelativistic heavy ion collisions*, Phys. Rev. C **59**, 1585 (1999), doi:10.1103/PhysRevC.59.1585.

[13] K. Blum and M. Takimoto, *Nuclear coalescence from correlation functions*, Phys. Rev. C **99**, 044913 (2019), doi:10.1103/PhysRevC.99.044913.

[14] S. Mrówczyński, *Production of light nuclei in the thermal and coalescence models*, Acta Phys. Pol. B **48**, 707 (2017), doi:10.5506/APhysPolB.48.707.

[15] S. Mrówczyński, *Sum rule of the correlation function*, Phys. Lett. B **345**, 393 (1995), doi:10.1016/0370-2693(94)01631-L.

[16] S. Acharya et al., *Production of light (anti)nuclei in pp collisions at $\sqrt{s}$ = 13 TeV*, J. High Energy Phys. **01**, 106 (2022), doi:10.1007/JHEP01(2022)106.

[17] K.-J. Sun, C. M. Ko and B. Dönigus, *Suppression of light nuclei production in collisions of small systems at the Large Hadron Collider*, Phys. Lett. B **792**, 132 (2019), doi:10.1016/j.physletb.2019.03.033.

[18] M. Kachelrieß, S. Ostapchenko and J. Tjemsland, *On nuclear coalescence in small interacting systems*, Eur. Phys. J. A **57**, 167 (2021), doi:10.1140/epja/s10050-021-00469-w.

[19] M. M. Kachelrieß, S. Ostapchenko and J. Tjemsland, *Revisiting cosmic ray antinuclei fluxes with a new coalescence model*, J. Cosmol. Astropart. Phys. 048 (2020), doi:10.1088/1475-7516/2020/08/048.

[20] L. Šerkšnytė et al., *Reevaluation of the cosmic antideuteron flux from cosmic-ray interactions and from exotic sources*, Phys. Rev. D **105**, 083021 (2022), doi:10.1103/PhysRevD.105.083021.

[21] M. Wolfgang Winkler and T. Linden, *Dark matter annihilation can produce a detectable antihelium flux through $\bar{\Lambda}_b$ decays*, Phys. Rev. Lett. **126**, 101101 (2021), doi:10.1103/PhysRevLett.126.101101.

[22] ALICE Collaboration, *Letter of intent for ALICE 3: A next generation heavy-ion experiment at the LHC*, (arXiv preprint) doi:10.48550/arXiv.2211.02491.

[23] A. E. Vladimirov, S. W. Digel, G. Jóhannesson, P. F. Michelson, I. V. Moskalenko, P. L. Nolan, E. Orlando, T. A. Porter and A. W. Strong, *GALPROP WebRun: An internet-based service for calculating galactic cosmic ray propagation and associated photon emissions*, Comput. Phys. Commun. **182**, 1156 (2011), doi:10.1016/j.cpc.2011.01.017.

[24] F. Binon et al., *Absorption cross-sections of 25 GeV/c antideuterons in Li, C, Al, Cu and Pb*, Phys. Lett. B **31**, 230 (1970), doi:10.1016/0370-2693(70)90112-7.

[25] S. P. Denisov et al., *Measurements of antideuteron absorption and stripping cross sections at the momentum 13.3 GeV/c*, Nucl. Phys. B **31**, 253 (1971), doi:10.1016/0550-3213(71)90229-X.

[26] S. Acharya et al., *Measurement of the low-energy antideuteron inelastic cross section*, Phys. Rev. Lett. **125**, 162001 (2020), doi:10.1103/PhysRevLett.125.162001.

[27] S. Acharya et al., *Measurement of anti-^{3}He nuclei absorption in matter and impact on their propagation in the Galaxy*, Nat. Phys. **19**, 61 (2022), doi:10.1038/s41567-022-01804-8.

[28] L. Tolos and L. Fabbietti, *Strangeness in nuclei and neutron stars*, Prog. Part. Nucl. Phys. **112**, 103770 (2020), doi:10.1016/j.ppnp.2020.103770.

[29] L. Fabbietti, V. M. Sarti and O. V. Doce, *Study of the strong interaction among hadrons with correlations at the LHC*, Annu. Rev. Nucl. Part. Sci. **71**, 377 (2021), doi:10.1146/annurev-nucl-102419-034438.

[30] S. Acharya et al., *Unveiling the strong interaction among hadrons at the LHC*, Nature **588**, 232 (2020), doi:10.1038/s41586-020-3001-6.

[31] K. Sasaki et al., *$\Lambda\Lambda$ and $N\Xi$ interactions from lattice QCD near the physical point*, Nucl. Phys. A **998**, 121737 (2020), doi:10.1016/j.nuclphysa.2020.121737.